

Engineering the electronic, magnetic and gap-related properties of the quaternary half-metallic Heusler alloys

K Özdoğan†, E Şaşıoğlu‡, and I Galanakis§

† Department of Physics, Gebze Institute of Technology, Gebze, 41400, Kocaeli, Turkey

‡ Institut für Festkörperforschung, Forschungszentrum Jülich, D-52425 Jülich, Germany and Fatih University, Physics Department, 34500, Büyükçekmece, İstanbul, Turkey

§ Department of Materials Science, School of Natural Sciences, University of Patras, GR-26504 Patra, Greece

E-mail:

kozdogan@gyte.edu.tr, e.sasioglu@fz-juelich.de, galanakis@upatras.gr

Abstract. We review the electronic and magnetic properties of the quaternary full Heusler alloys of the type $\text{Co}_2[\text{Cr}_{1-x}\text{Mn}_x][\text{Al}_{1-y}\text{Si}_y]$ employing three different approaches : (i) the coherent potential approximation (CPA), (ii) the virtual crystal approximation (VCA), and (iii) supercell calculations (SC). All three methods give similar results and the local environment manifested itself only for small details of the density of states. All alloys under study are shown to be half-metals and their total spin moments follow the so-called Slater-Pauling behavior of the ideal half-metallic systems. We especially concentrate on the properties related to the minority-spin band-gap. We present the possibility to engineer the properties of these alloys by changing the relative concentrations of the low-valent transition metal and sp atoms in a continuous way. Our results show that for realistic applications, ideal are the compounds rich in Si and Cr since they combine large energy gaps (around 0.6 eV), robust half-metallicity with respect to defects (the Fermi level is located near the middle of the gap) and high values of the majority-spin density of states around the Fermi level which are needed for large values of the perfectly spin-polarized current in spintronic devices like spin-valves or magnetic tunnel junctions.

PACS numbers: 75.47.Np, 71.20.Be, 71.20.Lp

Submitted to: *J. Phys. D: Appl. Phys.*

1. Introduction

The rapid growth of the field of magnetoelectronics, also known as spintronics, brought to the attention of scientists new phenomena [1, 2, 3]. One of the most interesting concepts in spintronics is the half-metallicity [4, 5, 6, 7, 8, 9, 10]. Half-metals are hybrids between normal metals and semiconductors. The majority-spin band is crossed by the Fermi level as in a normal metal while the Fermi level falls within a gap in the minority-spin band as in semiconductors leading to a perfect 100% spin-polarization at the Fermi level [5]. Such compounds should have a fully spin-polarized current and be ideal spin injectors into a semiconductor, thus maximizing the efficiency of spintronic devices [11]. de Groot and his collaborators in 1983 were the first to predict the existence of half-metallicity in the case of the intermetallic semi-Heusler alloy NiMnSb [12] and the origin of the gap seems to be well understood [13, 14]. The half-metallic character of NiMnSb in single crystals seems to have been well-established experimentally. Infrared absorption [15] and spin-polarized positron-annihilation [16] gave a spin-polarization of $\sim 100\%$ at the Fermi level. First-principles electronic structure calculations were successful in explaining the origin of half-metallicity in Heusler alloys in terms of the hybridization between the d -orbitals of the transition metal atoms and as it was shown the half-metallicity is also closely related to the total spin magnetic moment in the unit cell [13]. However, in many other experiments on low-dimensional structures the half-metallicity has not been found since the properties which have been measured were surface and interface sensitive.

Although semi-Heuslers have initially monopolized the interest, the last years the interest has been shifted to the so-called full-Heusler compounds like Co_2MnAl . Webster was the first to synthesize such alloys already in 1971 [17]

and almost 20 years later it was argued in two papers by a Japanese group that they should be half-metals [18]. The emergence of the field of magnetoelectronics brought again at the center of scientific interest these alloys [19, 20] and first-principles calculations have explained the origin of half-metallicity, demonstrating also that the perfect half-metallic full Heusler alloys show the so-called Slater-Pauling behavior; the total spin moments in the unit cell, M_t in μ_B , equals the total number of valence electrons in the unit cell minus 24 since there are exactly 12 occupied minority-spin states [20]. This rule is of interest since it provides an easy way to connect half-metallicity with the total spin-moment in the unit cell which is easily determined using various experiments like SQUID measurements. Although several full-Heusler alloys have been shown to be half-metallic in their bulk form [20, 21], ab-initio calculations have shown that the surfaces [22] and interfaces of the full-Heusler compounds [23] lose their half-metallicity (Hashemifar and collaborators have shown that it is possible to restore half-metallicity at some surfaces [24]). Except interface states also temperature driven excitations [25, 26, 27] and defects [28, 29] seem to destroy half-metallicity. Also some other important aspect of these alloys like the orbital magnetism [30], the doping [31], the structural stability [36], the appearance of ferrimagnetism [32, 33, 34] and antiferromagnetism [35] and the interplay of exchange interactions [37, 38] have been addressed in literature.

Over the last two years the interest in full-Heusler alloys containing cobalt has been focused on the so-called quaternary Heusler alloys, which are found to present half-metallicity as long as the corresponding perfect parent compounds are half-metals [39, 40]. Several authors studied the properties of $\text{Co}_2[\text{Cr}_{1-x}\text{Fe}_x]\text{Al}$ as a function of the concentration x [41, 42] as well as the $\text{Co}_2[\text{Mn}_{1-x}\text{Fe}_x]\text{Si}$

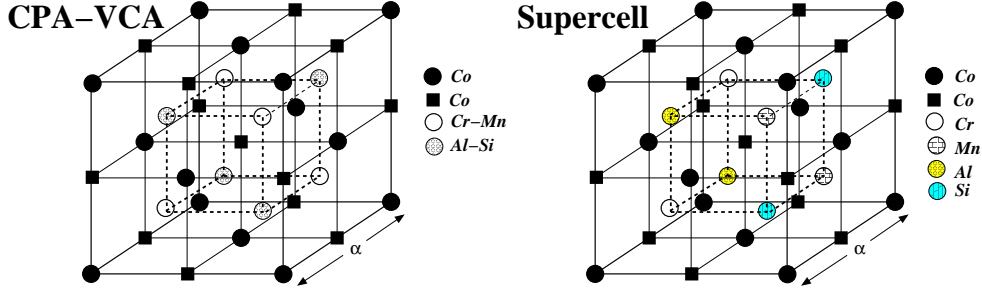


Figure 1. Schematic representation of the structure used for the $\text{Co}_2[\text{Cr}_{0.5}\text{Mn}_{0.5}][\text{Al}_{0.5}\text{Si}_{0.5}]$ alloy. On the left the structure used for the CPA and VCA calculations. In CPA the Cr-Mn site is occupied by Cr atoms with a probability of 50% and by Mn atoms with a probability of 50% and the Al-Si site is also occupied by both Al and Si atoms with 50% probability for each one. In VCA, the Cr-Mn site is occupied by a pseudoatom with a fractional number of valence electrons (24.5 electrons) and the Al-Si site by a pseudoatom with 13.5 valence electrons. The unit cell for both CPA and VCA calculations contains four sites. On the right panel we present the structure for the supercell calculations where we take a double unit cell with respect to VCA and CPA containing eight atoms ($\text{Co}_4\text{CrMnAlSi}$ compound). In the case where x and/or y take 0.25 or 0.75 as a value we have a unit cell with 16 atoms for the supercell calculations. Note also that there are two inequivalent Co sites in all cases which have the same environment rotated by $\pi/2$.

alloys [43] due to the fact that ab-initio calculations, including the on-site Coulomb repulsion (the so-called Hubbard U), have shown that Co_2FeSi can reach a total spin magnetic moment of $6 \mu_B$ which is the largest known spin moment for a half-metal [44, 45].

2. Description of present calculations

In a recent paper [40] we employed the full-potential nonorthogonal local-orbital minimum-basis band structure scheme (FPLO) [46, 47] to study the properties of the quaternary Heusler compounds $\text{Co}_2[\text{Cr}_{1-x}\text{Mn}_x]\text{Z}$, $\text{Co}_2[\text{Cr}_{1-x}\text{Fe}_x]\text{Z}$ and $\text{Co}_2[\text{Mn}_{1-x}\text{Fe}_x]\text{Z}$ where Z stands for Al, Ga, Si, Ge or Sn. In the case of $\text{Co}_2[\text{Cr}_{1-x}\text{Mn}_x]\text{Z}$ compounds it was shown by standard electronic structure calculations employing the local-spin-density approximation (LSDA) [48] that the compounds are half-metallic for all concentrations. This yielded the idea that if one studied the case of quinary al-

loys, allowing for an additional degree of freedom since also the chemical elements at the Z site are mixed, one can engineer in a continuous way the properties of these alloys related with the gap, thus the width of the minority-spin band gap, the position of the Fermi level and the majority-spin density of states at the Fermi level. Thus we decided to study the family of $\text{Co}_2[\text{Cr}_{1-x}\text{Mn}_x][\text{Al}_{1-y}\text{Si}_y]$ compounds since all four parent compounds are half-metals and such compounds seem feasible experimentally. We have used the experimental lattice constants for the perfect compounds containing Mn [49, 50], 0.5756 nm for Co_2MnAl and 0.565 nm for Co_2MnSi , and considered that the lattice constant varies linearly with the concentration y of the Al and Si atoms. We assumed that the substitution of Cr for Mn does not change the lattice constant since no evidence is known on the exact behavior of the lattice. This tactic is different than the one used in reference [39] where it was assumed that the lattice constant varies linearly with the concentration x of

the transition-metal atom but both methods give lattice constants within less than 1% difference and thus practically identical results.

To perform our calculations we have employed three different formalisms. Firstly the coherent-potential approximation (CPA) initially developed by Blackman and collaborators in 1971 [51]. In 1997 Koepernik et al have extended this formalism and have implemented it in a Linear Combination of Atomic Orbitals (LCAO) method [46] and later they expanded it to incorporate it in the FPLO method [47]. This was made possible due to the localized-character of the orbitals in this method which allows for a single-site representation of the space. In CPA each Y (or Z) site is occupied by both Cr and Mn (or Al and Si) atoms with a probability given by the respective concentration of each chemical type. Second, we used the so-called virtual crystal approximation (VCA). In VCA for the Y (or Z) site we substitute both Co and Mn atoms (or Al and Si atoms) with an atom with fractional number of electrons $(1 - x) * z^{Cr} + x * z^{Mn}$ (or $(1 - y) * z^{Al} + y * z^{Si}$) where z^{Cr} the number of electrons of Cr and similarly for the other chemical elements. Obviously in VCA only the total spin magnetic moment in the unit cell and the total DOS have a physical meaning since we can not project the properties of the pseudoatom on the different atoms. We represent the structures within both CPA and VCA in the left part of figure 1. The lattice is that of an fcc with four atoms as basis set along the diagonal: two Co atoms, one Cr-Mn site and one Al-Si site. Both CPA and VCA do not take into account the short-range interactions since the real crystal is replaced by one where each Y or Z site contains two different chemical type atoms. In reality this is not true and we performed supercell (SC) calculations to examine this effect. We present the structure in the right part of figure 1 in case that $x = 0.5$ and $y = 0.5$

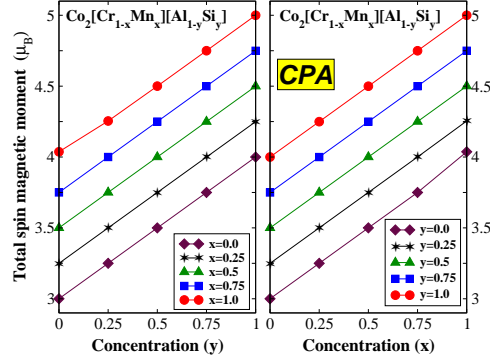


Figure 2. Left panel : Total moment in μ_B as a function of the concentration y in $\text{Co}_2[\text{Cr}_{1-x}\text{Mn}_x][\text{Al}_{1-y}\text{Si}_y]$ using the CPA method. Different lines correspond to constant values of x . Right panel : similar to the left panel as a function of x with different lines corresponding to constant values of y . All compounds are half-metals showing the Slater-Pauling behavior.

where the unit cell contains eight atoms; in reality the correct chemical formula is $\text{Co}_2\text{CrMnAlSi}$. In case that at least one of x or y is 0.25 or 0.75 the unit cell contains 16 atoms. To compare between the three different approaches when we present the total density of states (DOS) or the total spin magnetic moments we always scale to a formula unit of four atoms.

Such an investigation of the gap-related properties of the Heusler alloys is of interest due to the large variety of applications of these alloys. Several experiments have been devoted to the study of the structural and magnetic properties of the quaternary Heusler alloys [52] and such films have been incorporated both in magnetic tunnel junctions [53] and spin-valves [54]. Quinary half-metallic full-Heusler alloys will provide an additional tool to tune the properties of these films and enhance the performance of the devices based on such films.

3. Total and atom-resolved spin magnetic moments

We will start our discussion on the quinary alloys discussing the magnetic spin moments. To present our results we discuss the trends as a function of the concentration x of the transition-metal atoms Cr and Mn keeping the concentration y of the sp atoms constant and afterwards as a function of y keeping x constant. This presentation allows for an easier discussion of the results. In figure 2 we have plotted the total spin moment in the unit cell in μ_B within the CPA approach. If the alloys under study are half-metals they should follow the Slater-Pauling behavior for the total spin moments, $M_t : M_t = Z_t - 24$ [20]. The total spin moment in μ_B is just the number of uncompensated spins and thus the number “24” arises from the 12 occupied minority spin states (for details see reference [20]). Z_t denotes the total mean number of valence electron and is given by the expression $Z_t = 2 * z^{Co} + (1-x) * z^{Cr} + x * z^{Mn} + (1-y) * z^{Al} + y * z^{Si}$ where z denotes the valence of each atom. As it is presented in figure 2 the values of the total spin moments are spotted on top of straight lines both when we plot the total moment as a function of y (left panel) or as a function of x (right panel). A close look on the figure reveals that all these straight lines follow the Slater Pauling behavior for the full-Heusler alloys. Co_2CrAl has 27 electrons and an ideal total spin moment of $3 \mu_B$ which coincides with the calculated one. As we substitute 25% of the Cr atoms by Mn ($x=0.25$) we increase the total spin moment by $0.25 \mu_B$ each time reaching a value of $4 \mu_B$ for Co_2MnAl . Also at each step when we substitute 25% of the Si atoms for Al again we increase the number of valence electrons by 0.25 and thus the total spin moment increases also by $0.25 \mu_B$ at each step reaching the $4 \mu_B$ for Co_2CrSi and $5 \mu_B$ for Co_2MnSi .

In figures 3, 4 and 5 we have

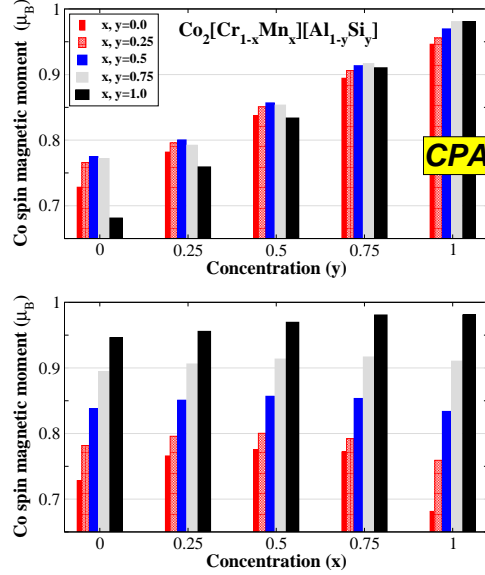


Figure 3. Top panel : Co-resolved spin magnetic moment in μ_B as a function of the concentration y in $Co_2[Cr_{1-x}Mn_x][Al_{1-y}Si_y]$ using the CPA method. Different bars correspond to different values of x . Bottom panel : similar to the top panel as a function of x with different bars corresponding to different values of y .

plotted the atom resolved spin moments for the transition metal atoms Co, Cr and Mn, respectively, within the CPA approximation. In each figure we present the moment as a function of the concentration y in the upper panel with different bars corresponding to different x and as a function of x in the lower panel with different bars corresponding to different values of y . We do not present the spin moments of the sp atoms since they are very small and negative (around $-0.1 \mu_B$). The negative sign arises from the p states. The minority bonding p states are completely occupied while the majority bonding ones extend much more in energy crossing the Fermi level resulting in an excess of minority p states with respect to the majority ones and thus

a negative spin moment. The behavior of the *sp* atoms is extensively discussed in references [5] and [20] and is independent of the *x* and *y* concentrations.

For the Co spin moments in figure 3 it is obvious from the upper panel that the Co spin moment depends on the *y* concentrations of the *sp* atoms. When *y* = 0 and the compounds contain only Al, the Co spin moments are quite small around 0.7-0.75 μ_B . When 25% of the Al atoms are substituted by Si, the Co spin moments increase and reach the 0.8 μ_B . When *y* = 0.5 the spin moments are around 0.85 μ_B and when *y* = 1.0 and the compounds contain only Si, the Co spin moments are around 0.95 μ_B . Thus in general as we increase the concentration of the Si atoms by 25% the Co spin moment increases by 0.05 μ_B . Obviously the concentration of the Cr and Mn atoms does not affect the Co spin moment as can be seen in figure 3. The substitution of Cr by Mn does not change the hybridization of the *d*-orbitals of the Co atoms with the *d*-orbitals of the lower-valence transition metal atoms, Cr and Mn, and thus the Co spin moment is not affected by the *x* concentration. On the other hand when we change the concentrations 1 - *y* and *y* of the Al and Si atoms, the extra electronic charge occupies majority spin electronic states of the transition metal atoms as in a rigid band model and increases the spin moment of all transition-metal atoms Co, Cr and Mn.

In figures 4 and 5 we present the spin moments of the Cr and Mn atoms scaled to one atom. The conclusions drawn for the Co spin magnetic moments hold generally also for the Mn and Cr atoms although the fluctuations are more important than for the Co atoms. Both Cr and Mn spin magnetic moments depend mainly on the concentration 1 - *y* and *y* of the Al and Si atoms. Mn spin moment starts from around 2.8 μ_B for *y* = 0 corresponding to the compounds

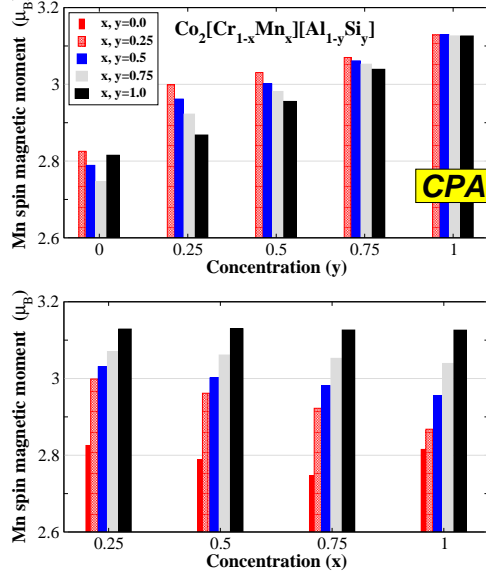


Figure 4. Same as Fig. 3 for the Mn atoms. The spin magnetic moment has been scaled to one Mn atom.

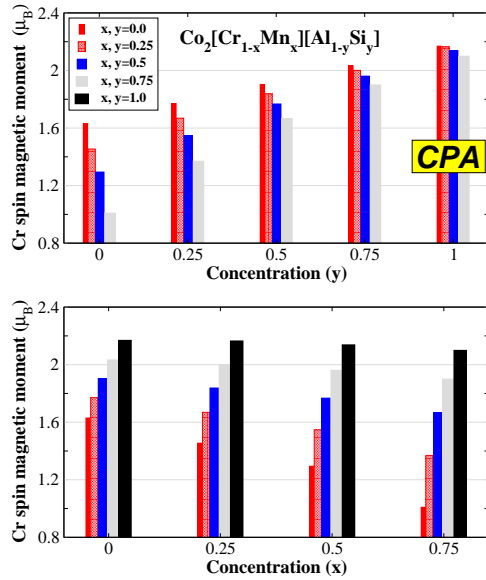


Figure 5. Same as Fig. 3 for the Cr atoms. The spin magnetic moment has been scaled to one Cr atom.

containing only Al and goes up to $3.1 \mu_B$ for $y = 1$ corresponding to the compounds where only Si is present. Similarly the Cr spin moments reach a value of around $2.1 \mu_B$ for the exclusively Si-based alloys ($y = 1$). When $y = 0$ or $y = 0.25$ the Cr spin moment present large fluctuations with respect to the x concentration being $1.6 \mu_B$ for Co_2CrAl and $0.9 \mu_B$ for $\text{Co}_2[\text{Cr}_{0.75}\text{Mn}_{0.25}]\text{Al}$. This behavior of the Cr spin moments has been explained in reference [32] where it was attributed to the pinning of the Fermi level in a narrow band created by the Cr triple degenerated majority t_{2g} electrons which overlaps strongly with the double-degenerated e_g majority states, contrary to the behavior of the Mn atoms [33]. As shown in [32] a small shift of the Fermi level results in large changes of the Cr spin moments. When we increase the concentration in Si atoms, the extra electrons push the Cr majority states lower in energy and thus the Cr spin magnetic moment is insensitive to the exact position of the Fermi level and thus the Cr spin moment is the same for all compounds with different x value but the same y value when $y = 0.5, 0.75$ or 1.0 (compounds rich in Si).

Up to now we have discussed the spin moments resulting for the CPA approach. In table 1 we have gathered the total and spin magnetic moments from all three SC, CPA and VCA calculations as a function of the concentrations x and y . For the SC we have scaled the moment to a unit cell of 4 atoms in order to compare them with the other two methods although for the calculations we have used a unit cell of 8 or 16 atoms depending on the values of the concentrations. Our first remark concerns the total spin magnetic moments in the third column. We have included just one value since all three methods predict for all compounds the half-metallic character and thus a total spin moment in agreement with the Slater-Pauling behavior. The most

important feature of this table is the atom-resolved spin moments within the supercell calculations with respect to the CPA approach. SC takes into account the local-effects (short-range interactions) contrary to CPA which is a mean-field theory taking into account only the long-range order. The atom-resolved spin magnetic moments are practical the same for all three transition metal elements, Co, Cr and Mn, irrespectively of the x and y concentrations within both CPA and SC. Thus for the full-Heusler alloys under study the short-range interactions have a minimal influence on the electronic structure of these alloys and these alloys can be accurately described by mean-field theories like CPA. Although this result seems astonishing, mainly due to our experience from other alloys, we should not forget that Heusler alloys are close-packed systems of very high symmetry in all directions. Their properties are largely governed by symmetry arguments (like the origin of the gap or the fixed number of minority occupied states [20]) and substitution of an atom by one of a neighboring chemical element only marginally affects the properties of these compounds. This argument is also supported by the VCA calculations. The substitution of the crystal by a virtual one with atoms of fractional electronic charge gives the same total spin moment and almost identical Co spin moments with respect to both SC and the more sophisticated mean-field theory of CPA. Thus Co atoms are not really sensitive to their local environment as long as the symmetry is not broken and each Co atom has four low-valence transition metal atoms and four sp atoms as first neighbors. In the table we include also the spin moments of the pseudoatoms within VCA although they have no physical meaning.

Table 1. Calculated spin magnetic moments in μ_B using a supercell construction for the $\text{Co}_2[\text{Cr}_{1-x}\text{Mn}_x][\text{Al}_{1-y}\text{Si}_y]$ as a function of the x and y concentrations. We do not present the spin moments of the Al and Si atoms since they are very small (around $-0.10 \mu_B$ for all compounds). All compounds are half-metals and the total spin moment is the ideal one predicted by the Slater-Pauling rule (we have scaled the total spin moment to the elementary unit cell containing four atoms only; the unit cell in the supercell calculations contains either 8 or 16 atoms). In case that there are more than one inequivalent atom of the same chemical kind, we present the largest spin moment; the difference between this moment and the other moments of the same chemical type are less than $0.05 \mu_B$ in all cases. In parenthesis the calculated spin magnetic moments using the CPA approximation and in brackets using the VCA approximation. Note that within VCA we have a pseudoatom with 24.5 electrons instead of distinct Co and Mn atoms and we include these spin moments both in Co and Mn columns.

x	y	m^{Total}	m^{Co}		m^{Cr}		m^{Mn}	
			SC (CPA) [VCA]		SC (CPA) [VCA]		SC (CPA) [VCA]	
0.00	0.00	3.00	0.73 (0.73) [0.73]		1.63 (1.63) [1.63]		—	
0.00	0.25	3.25	0.78 (0.78) [0.79]		1.77 (1.76) [1.76]		—	
0.00	0.50	3.50	0.84 (0.84) [0.84]		1.90 (1.90) [1.90]		—	
0.00	0.75	3.75	0.90 (0.89) [0.90]		2.02 (2.03) [2.03]		—	
0.00	1.00	4.00	0.95 (0.95) [0.95]		2.17 (2.17) [2.17]		—	
0.25	0.00	3.25	0.73 (0.77) [0.68]		1.54 (1.45) [1.99]		2.98 (2.83) [1.99]	
0.25	0.25	3.50	0.78 (0.80) [0.76]		1.71 (1.67) [2.09]		2.97 (3.00) [2.09]	
0.25	0.50	3.75	0.88 (0.85) [0.82]		1.78 (1.84) [2.22]		2.95 (3.03) [2.22]	
0.25	0.75	4.00	0.90 (0.91) [0.87]		1.99 (2.00) [2.35]		3.12 (3.07) [2.35]	
0.25	1.00	4.25	0.95 (0.96) [0.92]		2.19 (2.16) [2.49]		3.10 (3.13) [2.49]	
0.50	0.00	3.50	0.72 (0.78) [0.66]		1.42 (1.29) [2.30]		2.92 (2.79) [2.30]	
0.50	0.25	3.75	0.83 (0.80) [0.72]		1.53 (1.55) [2.42]		2.88 (2.96) [2.42]	
0.50	0.50	4.00	0.85 (0.86) [0.79]		1.77 (1.77) [2.54]		3.03 (3.00) [2.54]	
0.50	0.75	4.25	0.90 (0.91) [0.85]		1.99 (1.96) [2.65]		3.12 (3.06) [2.65]	
0.50	1.00	4.50	0.96 (0.97) [0.91]		2.18 (2.14) [2.76]		3.12 (3.013) [2.76]	
0.75	0.00	3.75	0.71 (0.77) [0.63]		1.18 (1.00) [2.63]		2.88 (2.75) [2.63]	
0.75	0.25	4.00	0.78 (0.79) [0.71]		1.47 (1.37) [2.71]		2.91 (2.92) [2.71]	
0.75	0.50	4.25	0.85 (0.85) [0.80]		1.76 (1.67) [2.78]		2.99 (2.98) [2.78]	
0.75	0.75	4.50	0.90 (0.92) [0.87]		2.04 (1.90) [2.87]		3.05 (3.05) [2.87]	
0.75	1.00	4.75	0.97 (0.98) [0.93]		2.20 (2.10) [2.97]		3.12 (3.12) [2.97]	
1.00	0.00	4.00	0.68 (0.68) [0.68]		—		2.82 (2.82) [2.82]	
1.00	0.25	4.25	0.75 (0.76) [0.76]		—		2.87 (2.87) [2.87]	
1.00	0.50	4.50	0.83 (0.83) [0.83]		—		2.98 (2.96) [2.96]	
1.00	0.75	4.75	0.91 (0.91) [0.91]		—		3.09 (3.04) [3.04]	
1.00	1.00	5.00	0.98 (0.98) [0.98]		—		3.13 (3.13) [3.13]	

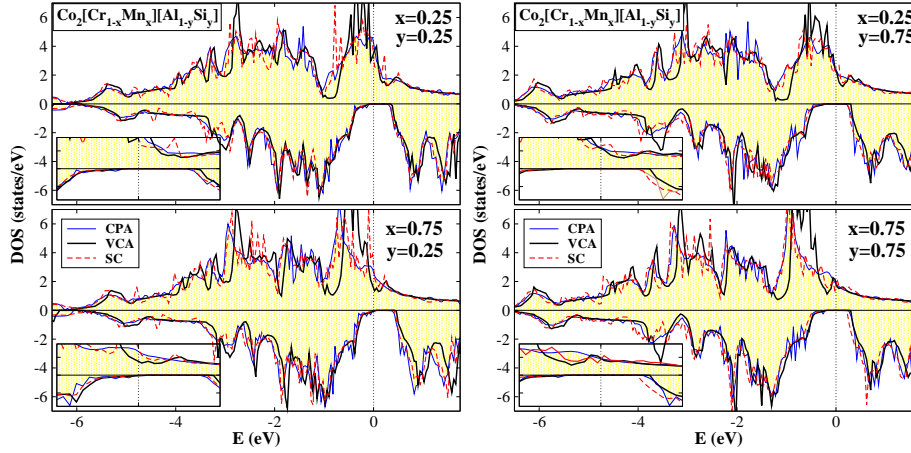


Figure 7. Total density of states (DOS) in states/eV for four different compounds using all three CPA, VCA and SC methods. Notice that the DOS for the SC calculations has been scaled to the elementary unit cell of 4 atoms although the unit cell contains either 8 or 16 atoms.

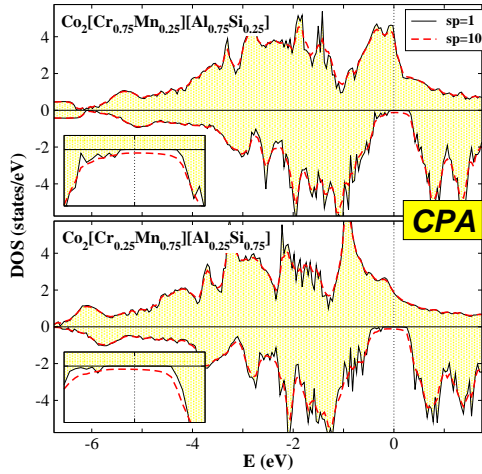


Figure 6. Total density of states (DOS) in states/eV for two different compounds using the CPA method and a smearing of 10^{-4} Hartree (sp1) and a smearing of 10^{-3} Hartree (sp10). The Fermi level has been chosen to be the zero of the energy axis.

4. Density of states

In the previous section we have discussed the half-metallicity of the quinary full-Heusler alloys in terms of the total

spin magnetic moments. In this section we will concentrate on the density of states (DOS). This is important since we will use the different DOS's to compute in detail the width of the gap, the position of the Fermi level and the majority-spin DOS at the Fermi level. Thus we should be able to define accurately the edges of the minority spin-gap. In VCA and SC calculations the gap is clearly defined but problems arise within CPA. When we compute the DOS within CPA we have to use a smearing for the DOS. Usually in previous publications with the same method (see references [32] and [33] for example) we have used a smearing of 10^{-3} Hartree but as shown in figure 6 for two different compounds this yields a region of very low DOS instead of a real gap due to tails from both gap-edges which overlap. Thus such a large smearing is not suitable for the gap-related properties. If we use a smearing of 10^{-4} Hartree the calculation of DOS is much more tedious but as shown in figure 6 we clearly get a region zero DOS and we are able to define the edges of the gap. Thus in all CPA calculations which we will present in the following we have used a broadening of 10^{-4} Hartree.

In figure 7 we have plotted the total DOS for four different compounds taking all possible combinations of x or $y = 0.25$ or 0.75 . All three methods CPA, VCA and SC produce similar total DOS (note that for SC we have scaled the DOS to a unit cell of four atoms). Especially CPA and SC give the same positions for the bands of all atoms and the DOS's almost coincide. VCA gives bands with the same mass center as CPA and SC but with different shape. This difference in shape with respect to CPA is expected since VCA is an oversimplified mean-field approach. If we concentrate on the region around the gap which we have blown up in the insets it is obvious that all three methods give similar description and similar values for the width of the gap and the position of the Fermi level. This will be analyzed in detail in the next section. These results support our statement in the previous section that short-range interactions are not important for the description of the magnetic and electronic properties of the half-metallic Heusler alloys when the disordered site contains atoms of neighboring chemical elements.

Finally in figures 8 and 9 we plot the total and atom-resolved DOS for the $\text{Co}_2[\text{Cr}_{0.5}\text{Mn}_{0.5}][\text{Al}_{0.5}\text{Si}_{0.5}]$ compounds within the CPA and SC approaches respectively. All DOS's have been scaled to one atom and we have multiplied the DOS of the sp atoms by a factor of 8 to make it visible. We do not present the VCA results since atomic DOS's lack any physical meaning within this approach. CPA due to the very small broadening used for the DOS's gives a more spiky DOS with respect to SC. The Co DOS produced by both methods is identical. In the majority spin DOS the deep in the DOS around -1.5 eV separates the occupied majority bonding d -states from the occupied antibonding majority d -states. As expected for the Cr and Mn atoms the DOS present several small differences but overall the bands present the

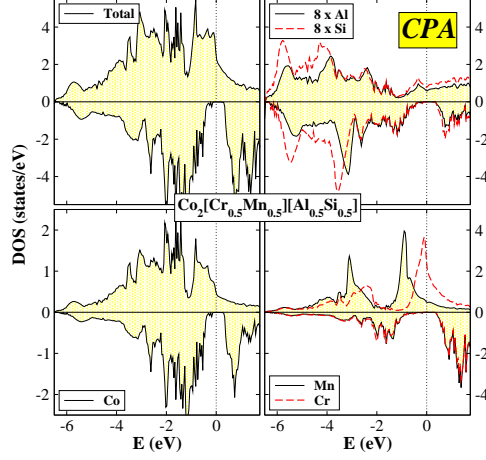


Figure 8. Total and atom resolved DOS of the $\text{Co}_2[\text{Cr}_{0.5}\text{Mn}_{0.5}][\text{Al}_{0.5}\text{Si}_{0.5}]$ alloy using the CPA method. The Al and Si DOS has been multiplied by a factor of 8. All atom-resolved DOS have been scaled to one atom

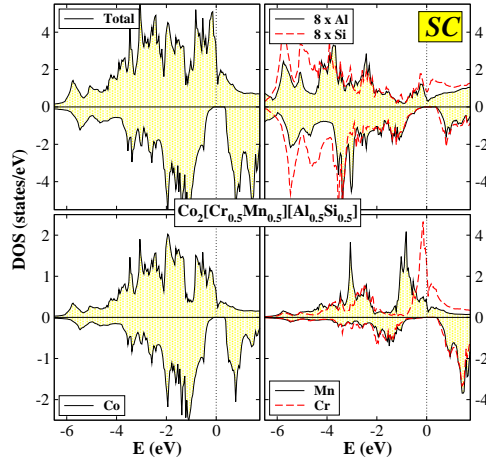


Figure 9. Same as Fig. 8 using the supercell construction. The total DOS has been scale as before to one elementary unit cell of four atoms.

same shape. CPA is a mean field theory and thus washes out any small picks in the DOS and for example we cannot distinguish between the t_{2g} and e_g majority states of Cr around the Fermi level. Contrary to CPA, SC carries also the short-range information and the Fermi level separates the t_{2g} and e_g majority states of Cr giving a band with a double peak. But overall the bands are located at the same energy within both CPA and SC and have the same width resulting in similar spin moments. CPA and SC give somehow more important differences in the DOS of the Al and Si atoms. But this DOS is one order of magnitude smaller than the DOS of the transition-metal atoms since it is mainly made up from p states which are spread over a wide energy range (the s states are located at around -9 eV and are not shown here). Thus these differences do not affect the electronic description given by the two methods and one can safely state that short-range interactions are not important for these alloys.

5. Gap-related properties

In the last part of our study, we present the properties related to the gap. In figure 10 we present the width of the gap as a function of the concentration y for constant values of x in the upper left panel within all three approaches CPA, VCA and SC and in the upper right panel the position of the Fermi level with respect to the left edge of the gap. In the lower panel we present the same information as a function of the concentration x of the transition metal atoms keeping the y constant. Note that for the width of the gap the vertical axis goes up to 0.7 eV while for the position of the Fermi level up to 0.5 eV. In table 2 we present the majority density of states exactly at the Fermi level. These results show the possibility of engineering the properties related to the gap just by changing the concentration in the low-transition

metal and the sp atoms. For realistic applications we need three conditions (i) we should have a quite large gap in order to have stable half-metallicity, (ii) the Fermi level should be as close as possible to the center of the gap for the half-metallicity to be robust since impurities and defects induce states at the edges of the gap [29], and (iii) the majority DOS at the Fermi level should be also high in order to produce significant spin-polarized current in real experiments.

The first remark concerning figure 10 is that all three methods give almost identical results for the width of the minority-spin gap. This enhances even further our argument in section 3 that short-range interaction taken into account in the supercell calculations are not significant for the full-Heusler alloys. In the case of the alloys rich in Si ($y=0.5, 0.75$ and 1.0) the width of the gap is constant and around 0.6 eV, while for the compounds rich in Al ($y=0.0$ and 0.25) the gap is around 0.4-0.5 eV and in the case of Co_2CrAl and Co_2MnAl alloys it almost vanishes. Thus for realistic applications compounds rich in silicon should be preferable since the gap-width should be large and more robust. From the low-left panel we can safely conclude with the exception of the compounds containing exclusively Al ($y = 0$) that the width of the gap is independent of the relative concentration of the Cr and Mn atoms ($1 - x$ and x respectively) as we keep constant the concentrations of the Al and Si atoms. The gap is defined by the relative position of the non-bonding occupied triple-degenerated t_{1u} and unoccupied double-degenerated e_u states which are exclusively located at the Co sites as shown in reference [20]. The position of these states does not depend on the exact energy position of the Cr and Mn d orbitals and thus the width of the gap does not depend on the relative concentration of these atoms.

Now we will discuss the behavior of

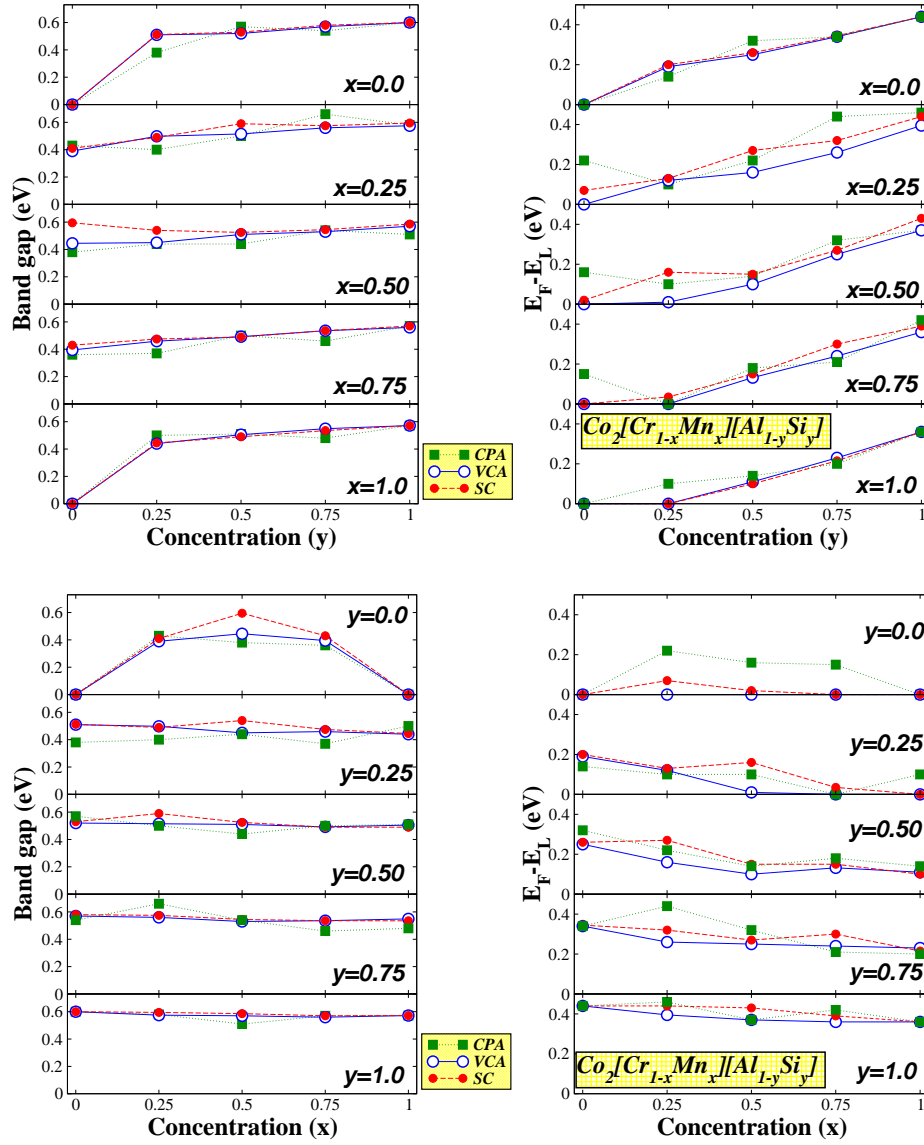


Figure 10. Upper panel : width of the band gap (left panel) and distance of Fermi level, E_F , from the left edge of the gap, E_L , (right panel) as a function of the concentration y keeping x constant using all three CPA, VCA and SC methods. Lower panel : same as upper panel as a function of x keeping y constant. Note that for the band-gap width the scale of the vertical axis is different than for the position of the Fermi level.

the Fermi level. The Fermi level contrary to the width of the gap is determined mainly by the energy extension of the majority p states of the sp atoms as it was discussed in reference [20]. This is clearly seen in the upper right panel of figure 10 where, when we keep x constant, the Fermi level is pushed higher in energy as we increase the concentration of the Si atoms with respect to the Al ones. The Fermi level is located almost at the left edge of the gap for the alloys containing only Al ($y=0$) and has a distance of ~ 0.4 eV from the left edge of the gap for the alloys containing only Si ($y=1$). Since the most interesting case are the alloys rich in Si with a gap around 0.6 eV, the ideal case is that the Fermi level is located at the middle of the gap with a distance of about 0.3 eV from both edges of the gap. This is the case when $y = 0.75$ and thus at the Z site 25% of the atoms are of Al chemical type and 75% of the Si chemical type. When $y = 0.5$ and the populations of Al and Si atoms are equal the Fermi level is located at around 0.2 eV from the left edge of the gap and thus half-metallicity should be more affected by disorder, defects and impurities.

Finally, we shall focus on the majority density of states presented in table 2. All three methods give comparable results but now the SC approach gives systematically a higher value than CPA or VCA with few exceptions. The DOS at the Fermi level is a small detail of the total DOS and the effect of the short-range interactions is larger than when we compare the DOS over the whole energy range or the spin moments where these small details are averaged and do not manifest their presence. As we have discussed in section 4 the DOS at the Fermi level is higher for the compounds rich in Cr, since for the Cr atoms the Fermi level crosses the majority d electrons while Mn atoms have practically all their d majority states occupied and the majority DOS at the Fermi level for the compounds contain-

Table 2. Calculated spin-up (majority) density of states in states/eV at the Fermi level for the $\text{Co}_2[\text{Cr}_{1-x}\text{Mn}_x][\text{Al}_{1-y}\text{Si}_y]$ as a function of the x and y concentrations with three different methods (i) the coherent potential approximation (CPA), (ii) the virtual crystal approximation (VCA), and (iii) using supercell calculations (SC). Note that for the SC case the total DOS has been scaled as before to an elementary unit cell of four atoms instead of 8 or 16 atoms of the unit cell.

x	y	CPA	VCA	SC
0.00	0.00	4.861	4.861	4.861
0.00	0.25	4.552	4.494	5.102
0.00	0.50	3.673	3.196	3.660
0.00	0.75	2.967	2.663	3.170
0.00	1.00	2.318	2.318	2.318
0.25	0.00	3.030	4.490	5.189
0.25	0.25	3.496	4.201	3.339
0.25	0.50	3.553	3.110	2.488
0.25	0.75	2.271	2.381	2.544
0.25	1.00	1.332	2.092	2.319
0.50	0.00	4.746	3.861	4.528
0.50	0.25	3.843	3.581	4.240
0.50	0.50	1.906	2.477	2.804
0.50	0.75	1.270	2.088	2.016
0.50	1.00	1.904	1.861	1.974
0.75	0.00	3.670	2.910	4.027
0.75	0.25	1.543	2.970	3.051
0.75	0.50	1.512	2.210	2.083
0.75	0.75	1.896	1.851	1.787
0.75	1.00	1.707	1.542	1.461
1.00	0.00	1.510	1.510	1.510
1.00	0.25	2.042	2.025	1.876
1.00	0.50	1.582	1.556	1.610
1.00	0.75	1.451	1.203	1.491
1.00	1.00	1.222	1.222	1.222

ing only Mn ($x = 1.0$) is one third the value for the compounds containing only Cr ($x = 0.0$). A second remark concerns the behavior of the majority DOS at the Fermi level with the concentration y of the sp atoms when we keep x constant. As we increase the population in Si the extra charge pushes the majority states lower in energy and thus the DOS at the Fermi level decreases considerably and for the compounds containing only Si ($y = 1.0$) the DOS at E_F is about 40-50% of the value for the Al alloys ($y = 0.0$). As discussed in the previous paragraphs for realistic applications we need compounds rich in Si which combine large a band-gap width with a Fermi level near the middle of the gap. From the discussion in this paragraph it is evident that we also need our compound to be rich in Cr in order to ensure a high value of DOS at the Fermi level.

6. Summary and conclusions

We have reviewed the electronic and magnetic properties of the quinary full Heusler alloys of the type $\text{Co}_2[\text{Cr}_{1-x}\text{Mn}_x][\text{Al}_{1-y}\text{Si}_y]$. For our study we have employed three different approaches the coherent potential approximation (CPA), the virtual crystal approximation (VCA) and supercell calculations (SC) to have information also for the short range interactions. All three methods gave similar results and the local environment manifested itself only for small details of the density of states.

All three approaches predicted that the alloys under study are half-metals for all x and y concentrations and their total spin moments follow the so-called Slater-Pauling behavior : the total spin magnetic moment in the unit cell in μ_B equals the number of valence electrons in the unit cell minus 24. The spin moment of the transition metal atoms were found to be almost insensitive to the relative concentrations of Cr and Mn elements while the sp atoms carried very small

antiparallel spin moments.

All three CPA, VCA and SC approaches yielded similar results for the properties related to the minority-spin band-gap. The width of the gap is determined by states exclusively localized at the Co sites and is insensitive to the Cr and Mn concentrations and is larger for the compounds rich in Si. The Fermi level is positioned at the left edge of the gap for the alloys containing only Al and as we increase the concentration in Si it is pushed higher in energy. The majority-spin density of states at the Fermi level takes larger values for the compounds rich in Cr and it drops as we increase the Si concentration.

We have shown the possibility to engineer the properties of the half-metallic Heusler alloys by changing the concentration of the low-valent transition metal and sp atoms in a continuous way. We conclude that for realistic applications ideal are the compounds rich in Si and Cr since they combine large energy gaps (around 0.6 eV), robust half-metallicity with respect to defects (the Fermi level is located near the middle of the gap) and high values of the majority-spin density of states around the Fermi level. Since such alloys are realized already experimentally in the form of thin films and multilayers and are incorporated in magnetoelectronic devices, like spin-valves or magnetic tunnel junctions, we expect our results to be of interest for the community of experimentalists in the field of spintronics and to stimulate further experimental interest on these compounds.

References

- [1] Žutić I, Fabian J and Das Sarma A 2004 *Rev. Mod. Phys.* **76** 323
- [2] Felser C, Fecher G H and Balke B 2007 *Angew. Chem. Int. Ed.* **46** 668
- [3] Zabel H 2006 *Materials Today* **9** 42
- [4] Galanakis I and Dederichs P H (eds): Half-metallic alloys: fundamentals and

- applications, Springer Lecture notes in Physics vol. 676, Springer (2005).
- [5] Galanakis I, Mavropoulos Ph and Dederichs P H 2006 *J. Phys. D: Appl. Phys.* **39** 765
 - [6] Galanakis I and Mavropoulos Ph 2007 *J. Phys.: Condens. Matter* **19** 315213
 - [7] Bergmann A, Grabis J, Toperverg B P, Leiner V, Wolff M, Zabel H and West-erholt K 2005 *Phys. Rev. B* **72** 214403; Grabis J, Bergmann A, Nefedov A, West-erholt K and Zabel H 2005 *Phys. Rev. B* **72** 024437; *idem* 2005 *Phys. Rev. B* **72** 024438
 - [8] Schmalhorst J, Thomas A, Kämmerer S, Schebaum O, Ebke D, Sacher M D, Reiss G, Hütten A, Turchanin A, Golzhauser A and Arenholz E 2007 *Phys. Rev. B* **75** 014403; Ebke D, Schmalhorst J, Liu N-N, Thomas A, Reiss G and Hütten A 2006 *Appl. Phys. Lett.* **89** 162506; Kämmerer S, Thomas A, Hütten A and Reiss G 2004 *Appl. Phys. Lett.* **85** 79; Schmalhorst J, Kämmerer S, Sacher M, Reiss G, Hütten A and Scholl A 2004 *Phys. Rev. B* **70** 024426
 - [9] Telling N D, Keatley P S, van der Laan G, Hicken R J, Arenholz E, Sakuraba Y, Oogane M, Ando Y and Miyazaki T 2006 *Phys. Rev. B* **74** 224439; Sakuraba Y, Hattori M, Oogane M, Ando Y, Kato H, Sakuma A, Miyazaki T and Kubota H 2006 *Appl. Phys. Lett.* **88** 192508; Sakuraba Y, Nakata J, Oogane M, Ando Y, Kato H, Sakuma A, Miyazaki T and Kubota H 2006 *Appl. Phys. Lett.* **88** 022503; Sakuraba Y, Miyakoshi T, Oogane M, Ando Y, Sakuma A, Miyazaki T and Kubota H 2006 *Appl. Phys. Lett.* **89** 052508; Sakuraba Y, Nakata J, Oogane M, Kubota H, Ando Y, Sakuma A and Miyazaki T 2005 *Japan. J. Appl. Phys.* **44** L1100; Sakuraba Y, Nakata J, Oogane M, Kubota H, Ando Y, Sakuma A and Miyazaki T 2005 *Japan. J. Appl. Phys.* **44** 6535
 - [10] Dong X Y, Adelman C, Xie J Q, Palmström C J, Lou X, Strand J, Crowell P A, Barnes J=P and Petford-Long A K 2005 *Appl. Phys. Lett.* **86** 102107; Wang H, Sato A, Saito K, Mitani S, Takanashi K and Yakushiji K 2007 *Appl. Phys. Lett.* **90** 142510; Tezuka N, Ikeda N, Miyazaki A, Sugimoto S, Kikuchi M and Inomata K 2006 *Appl. Phys. Lett.* **89** 112514; Yakushiji K, Saito K, Mitani S, Takanashi K, Takahashi Y K and Hono K 2006 *Appl. Phys. Lett.* **88** 222504
 - [11] Wolf S A, Awschalom D D, Buhrman R A, Daughton J M, von Molnár S, Roukes M L, Chtchelkanova A Y and Treger D M 2001 *Science* **294** 1488
 - [12] de Groot R A, Mueller F M, van Engen P G and Buschow K H J 1983 *Phys. Rev. Lett.* **50** 2024
 - [13] Galanakis I, Papanikolaou N and Dederichs P H 2002 *Phys. Rev. B* **66** 134428
 - [14] Jung D, Koo H-J and Whangbo M-H 2000 *J. Mol. Struct. (Theochem)* **527** 113; Nanda B R K and Dasgupta S 2003 *J. Phys.: Condens. Matter* **15** 7307; Kohler J, Deng S Q, Lee C and Whangbo M H 2007 *Inorganic Chemistry* **46** 1957; Offernes L, Ravindran P and Kjekshus A 2007 *J. All. Comp.* **439** 37; Yamasaki A, Chioncel L, Lichtenstein A I and Andersen O K 2006 *Phys. Rev. B* **74** 024419
 - [15] Kirillova M N, Makhnev A A, Shreder E I, Dyakina V P and Gorina N B 1995 *Phys. Status Solidi (b)* **187** 231
 - [16] Hanssen K E H M and Mijnders P E 1990 *Phys. Rev. B* **34** 5009; Hanssen K E H M, Mijnders P E, Rabou L P L M and K.H.J. Buschow K H J 1990 *Phys. Rev. B* **42** 1533
 - [17] Webster P J 1971 *J. Phys. Chem. Solids* **32** 1221
 - [18] Ishida S, Fujii S, Kashiwagi S and Asano S 1995 *J. Phys. Soc. Japan* **64** 2152; Fujii S, Sugimura S, Ishida S and Asano S 1990 *J. Phys.: Condens. Matter* **2** 8583
 - [19] Picozzi S, Continenza A and Freeman A J 2002 *Phys. Rev. B* **66** 094421
 - [20] Galanakis I, Papanikolaou N and Dederichs P H 2002 *Phys. Rev. B* **66** 174429
 - [21] Chen X-Q, Podloucky R and Rogl P 2006 *J. Appl. Phys.* **100** 113901
 - [22] Galanakis I 2002 *J. Phys.: Condens. Matter* **14** 6329; Galanakis I 2005 *J. Magn. Magn. Mater.* **288** 411; Lezaic M, Galanakis I, Bihlmayer G and Blügel S 2005 *J. Phys.: Condens. Matter* **17**, 3121; Jenkins S J 2004 *Phys. Rev. B* **70** 245401; Jenkins S J and King D A 2001 *Surf. Sci.* **494** L793
 - [23] Nagao K, Miura Y and Shirai M 2006 *Phys. Rev. B* **73** 104447; I. Galanakis I 2004 *J. Phys.: Condens. Matter* **16** 8007; Galanakis I, Ležaić M, Bihlmayer G and Blügel S 2005 *Phys. Rev. B* **71**, 214431; Wijs G A and de Groot R A 2001 *Phys. Rev. B* **64** R020402
 - [24] Hashemifar S J, Kratzer P and Scheffler M 2005 *Phys. Rev. Lett.* **94** 096402
 - [25] Chioncel L, Arrigoni E, Katsnelson M I and Lichtenstein A I 2006 *Phys. Rev. Lett.* **96** 137203; Chioncel L, Katsnelson M I, de Groot R A and Lichtenstein A I 2003 *Phys. Rev. B* **68** 144425
 - [26] Ležaić M, Mavropoulos Ph, Enkovaara J, Bihlmayer G and Blügel S 2006 *Phys. Rev. Lett.* **97** 026404
 - [27] Skomski R and Dowben P A 2002 *Europhys.*

- Lett.* **58** 544
- [28] Picozzi S, Continenza A and Freeman A J 2004 *Phys. Rev. B* **69** 094423
- [29] Orgassa D, Fujiwara H, Schulthess T C and Butler W H 1999 *Phys. Rev. B* **60** 13237; Alling B, Shallcross S and Abrikosov I A 2006 *Phys. Rev. B* **73** 064418; Attema J J, Fang C M, Chioncel L, de Wijs G A, Lichtenstein A I and de Groot R A 2004 *J. Phys.: Condens. Matter* **16** S5517; Carey M J, Block T and Gurney B A 2004 *Appl. Phys. Lett.* **85** 4442
- [30] Galanakis I 2005 *Phys. Rev. B* **71** 012413; Sargolzaei M, Richter M, Koepnick K, Opahle I, Eschrig H and Chaplygin I 2006 *Phys. Rev. B* **74** 224410
- [31] Galanakis I, Özdoğan K, Aktaş B and Şaşıoğlu E 2006 *Appl. Phys. Lett.* **89** 042502; Özdoğan K, Şaşıoğlu E, Aktaş B and Galanakis I 2006 *Phys. Rev. B* **74** 172412
- [32] Özdoğan K, Galanakis I, Şaşıoğlu E and Aktaş B 2007 *Phys. Status Solidi (RRL)* **1** 95
- [33] Özdoğan K, Galanakis I, Şaşıoğlu E and Aktaş B 2007 *Solid State Commun.* **142** 492
- [34] Özdoğan K, Galanakis I, Şaşıoğlu E and Aktaş B 2006 *J. Phys.: Condens. Matter* **18** 2905; Şaşıoğlu E, Sandratskii L M and Bruno P 2005 *J. Phys.: Condens. Matter* **17** 995; Ishida S, Asano S and Ishida J 1984 *J. Phys. Soc. Japan* **53** 2718; Weht R and Pickett W E 1999 *Phys. Rev. B* **60** 13006
- [35] Galanakis I, Özdoğan K, Şaşıoğlu E and Aktaş B 2007 *Phys. Rev. B* **75** 172405; Galanakis I, Özdoğan K, Şaşıoğlu E and Aktaş B 2007 *Phys. Rev. B* **75** 092407; van Leuken H and de Groot R A 1995 *Phys. Rev. Lett.* **74** 1171; Wurmehl S, Kandpal H C, Fecher G H and Felser C 2006 *J. Phys.: Condens. Matter* **18** 6171
- [36] Block T, Carey M J, Gurney B A and Jepsen O 2004 *Phys. Rev. B* **70** 205114
- [37] Şaşıoğlu E, Sandratskii L M, Bruno P and Galanakis I 2005 *Phys. Rev. B* **72** 184415
- [38] Kurtulus Y, Dronskowski R, Samolyuk G D and Antropov V P 2005 *Phys. Rev. B* **71** 014425
- [39] Galanakis I 2004 *J. Phys.: Condens. Matter* **16** 3089
- [40] Özdoğan K, Aktaş B, Galanakis I and Şaşıoğlu E 2007 *J. Appl. Phys.* **101** 073910
- [41] Antonov V N, Dürr H A, Kucherenko Yu, Bekenov L V and Yaresko A N 2005 *Phys. Rev. B* **72** 054441
- [42] Miura Y, Nagao K and Shirai M 2004 *Phys. Rev. B* **69** 144413
- [43] Balke B, Fecher G H, Kandpal H C, Felser C, Kobayashi K, Ikenaga E, Kim J-J and Ueda S 2006 *Phys. Rev. B* **74** 104405
- [44] Kandpal H M, Fecher G H, Felser C and Schönhausen G 2006 *Phys. Rev. B* **73** 094422
- [45] Wurmehl S, Fecher G H, Kandpal H C, Ksenofontov V, Felser C and Lin H J 2006 *Appl. Phys. Lett.* **88** 032503
- [46] Koepnick K, Velicky B, Hayn R and Eschrig H 1998 *Phys. Rev. B* **58** 6944
- [47] Koepnick K and Eschrig H 1999 *Phys. Rev. B* **59** 3174
- [48] Vosko S H, Wilk L and Nusair N 1980 *Can. J. Phys.* **58** 1200; Hohenberg P and Kohn W 1964 *Phys. Rev.* **136** B864; Kohn W and Sham L J 1965 *Phys. Rev.* **140** A1133
- [49] Webster P J and Ziebeck K R A, in *Alloys and Compounds of d-Elements with Main Group Elements. Part 2.*, edited by H.R.J. Wijn, Landolt-Börnstein, New Series, Group III, Vol. 19, Pt.c (Springer-Verlag, Berlin), pp. 75-184
- [50] Ziebeck K R A and Neumann K -U, in *Magnetic Properties of Metals*, edited by H. R. J. Wijn, Landolt-Börnstein, New Series, Group III, Vol. 32/c (Springer, Berlin), 2001, pp. 64-414
- [51] Blackman J A, Esterling D M and Berk N F 1971 *Phys. Rev. B* **4** 2412
- [52] Rata A D, Braak H, Bürgler D E and Schneider C M 2007 *Appl. Phys. Lett.* **90** 162512; Rata A D, Braak H, Bürgler D E, Cramm S and Schneider C M 2006 *EJP B* **52** 445; Kallmayer M, Schneider H, Jakob G, Elmers H J, Kroth K, Kandpal H C, Stumm U and Cramm S 2006 *Appl. Phys. Lett.* **88** 072506; Karthik S V, Rajanikanth A, Takahashi Y K, Okhubo T and Hono K 2006 *Appl. Phys. Lett.* **89** 052505; Fecher G H, Kandpal H C, Wurmehl S, Morais J, Lin H-J, Elmers H-J, Schönhausen G and Felser C 2005 *J. Phys.: Condens. Matter* **17** 7237; Umetsu R Y, Kobayashi K, Fujita A, Oikawa K, Kainuma R, Ishida K, Endo N, Fukamichi K and Sakuma A 2005 *Phys. Rev. B* **72** 214412; Kobayashi K, Umetsu R Y, Kainuma R, Ishida K, Oyamada T, Fujita A and Fukamichi K 2004 *Appl. Phys. Lett.* **85** 4684; Elmers H J, Fecher G H, Valdaitsev D, Nepijko S A, Gloskovskii A, Jakob G, Schönhausen G, Wurmehl S, Block T, Felser C, Hsu P C, Tsai W L and Cramm S 2003 *Phys. Rev. B* **67** 104412
- [53] Marukame T, Ishikawa T, Matsuda K-I, Uemura T and Yamamoto M 2006 *Appl. Phys. Lett.* **88** 262503; Marukame T, Kasahara T, Matsuda K, Uemura T and Yamamoto M 2005 *Japan. J. Appl. Phys.* **44** L521

- [54] Kelekar R and Klemens B 2005 *Appl. Phys. Lett.* **86** 232501